



Original Article

Utility of fiducial markers for target positioning in proton radiotherapy of oesophageal carcinoma



Rudi Apolle^{a,b,*}, Stefan Brückner^c, Susanne Frosch^d, Maximilian Rehm^d, Julia Thiele^{b,d}, Chiara Valentini^{b,d}, Fabian Lohaus^{b,d}, Jana Babatz^c, Daniela E. Aust^e, Jochen Hampe^c, Esther G.C. Troost^{a,b,d,f,g}

^aHelmholtz-Zentrum Dresden – Rossendorf, Institute of Radiooncology – OncoRay; ^bOncoRay – National Center for Radiation Research in Oncology, Faculty of Medicine and University Hospital Carl Gustav Carus, Technische Universität Dresden, Helmholtz-Zentrum Dresden – Rossendorf; ^cDepartment of Internal Medicine I, University Hospital Carl Gustav Carus, Dresden; ^dDepartment of Radiotherapy and Radiation Oncology, Faculty of Medicine and University Hospital Carl Gustav Carus, Technische Universität Dresden; ^eInstitute for Pathology and Tumour and Normal Tissue Bank of the University Cancer Center (UCC), University Hospital Carl Gustav Carus, Medical Faculty, Technische Universität Dresden; ^fGerman Cancer Consortium (DKTK), Partner Site Dresden, and German Cancer Research Center (DKFZ), Heidelberg; and ^gNational Center for Tumor Diseases (NCT), Partner Site Dresden, Germany; German Cancer Research Center (DKFZ), Heidelberg, Germany; Faculty of Medicine and University Hospital Carl Gustav Carus, Technische Universität Dresden, Dresden, Germany, and; Helmholtz Association / Helmholtz-Zentrum Dresden-Rossendorf (HZDR), Dresden, Germany

ARTICLE INFO

Article history:

Received 6 September 2018
 Received in revised form 11 December 2018
 Accepted 17 December 2018
 Available online 14 January 2019

Keywords:

Oesophageal carcinoma
 Proton therapy
 Image-guided radiotherapy
 Fiducial markers

ABSTRACT

Background and purpose: Oesophageal mobility relative to bony anatomy is a major source of geometrical uncertainty in proton radiotherapy of oesophageal carcinoma. To mitigate this uncertainty we investigated the use of implanted fiducial markers for direct target verification in terms of safety, visibility, and stability.

Materials and methods: A total of 19 helical gold markers were endoscopically implanted in ten patients. Their placement at the proximal and distal tumour borders was compared to tumour demarcations derived from [18F]Fluorodeoxyglucose positron emission tomography, their visibility quantified via the contrast-to-noise ratio on daily orthogonal X-ray imaging, and their mobility relative to bony anatomy analysed by means of retrospective triangulation.

Results: Marker implantation proceeded without complications, but the distal tumour border could not be reached in two patients. Marker locations corresponded reasonably well with metabolic tumour edges (mean: 5.4 mm more distally). Marker visibility was limited but mostly sufficient (mean contrast-to-noise ratio: 1.5), and sixteen markers (84%) remained in situ until the end of treatment. Overall, marker excursions from their planned position were larger than 5(10) mm in 59(17)% of all analysed fractions. On one occasion severe target displacement was only identified via markers and was corrected before treatment delivery.

Conclusion: Implanted helical gold fiducial markers are a safe and reliable method of providing target-centric positioning verification in proton beam therapy of oesophageal carcinoma.

© 2018 Elsevier B.V. All rights reserved. Radiotherapy and Oncology 133 (2019) 28–34

Tri-modality treatment consisting of neo-adjuvant radiochemotherapy (nRCT) followed by surgery is standard of care for resectable locally advanced oesophageal carcinoma. Its superiority over surgery alone has been demonstrated most strikingly by the CROSS study, which found significantly increased overall and progression-free survival [1,2]. In an attempt to further improve outcome after nRCT in oesophageal cancer patients or/and to pave the way to organ-preserving RCT employing higher radiation doses, particle therapy, in particular using protons, is the focus of attention. Proton therapy (PT) offers unique dosimetric character-

istics, which improve dose conformity at distal field edges where maximum dose deposition at the Bragg peak is followed by a sharp dose decline. While there is currently no data from randomised controlled trials comparing PT to photon-based radiotherapy (RT) techniques for oesophageal cancer, propensity-matched retrospective investigations have shown better survival rates with definitive RT and reduced postoperative complications in nRCT when delivering PT [3,4].

However, PT introduces geometrical uncertainties beyond those known from photon RT. The acuity of the distal dose fall-off and the underlying physical mechanism make it susceptible to changes in patient anatomy. Unless these uncertainties can be mitigated without introducing excessive safety margins, it will be hard to translate the physical advantages of PT into clinical benefit. Target

* Corresponding author at: OncoRay, National Center for Radiation Research in Oncology, Händelallee 26, 01309 Dresden, Germany.

E-mail address: rudi.apolle1@oncoray.de (R. Apolle).

positioning, in particular, is one aspect of treatment, which needs to be tightly controlled.

Oesophageal tumours show pronounced variability in daily target position, as well as significant intra-fractional motion [5–7]. Many PT facilities utilise orthogonal X-ray imaging for daily patient setup based on bony anatomy, but are unable to provide target-centric positioning due to its inherent lack of soft-tissue contrast. Implanted radiopaque fiducial markers can overcome this limitation and enable verification of target positioning to complement bony setup. They also allow for retrospective analyses of residual target positioning errors, which can be used to tailor safety margins to the uncertainties encountered at a particular department. Apart from treatment delivery they also benefit various aspects of treatment planning and response assessment by first making the location of endoscopic findings directly accessible in radiographic imaging and later serving as demarcations of original tumour extent on follow-up imaging and in resection specimen.

Here we report on the initial experience with one type of commercially available fiducial marker in ten patients with oesophageal cancer treated with neoadjuvant or definitive RCT using protons. Apart from safety, we analysed marker visibility on daily X-ray imaging, their stability, and mobility. Based thereupon we discuss a marker-based target position verification procedure, which can be straightforwardly implemented in routine clinical practice.

Materials and methods

Patient cohort

Patients were recruited into this pilot study between June 2017 and July 2018 with the aim of investigating marker implantation safety. Safety was assessed as absence of bleeding or perforation during post-implantation inspection and monitoring, and as absence of later stage adverse reactions, such as mediastinitis, at subsequent clinical observation during therapy and follow-up. The primary eligibility criterion was a histologically confirmed oesophageal carcinoma potentially amenable to curative treatment. This included locally advanced cases, as well as early-stage disease unsuitable for primary resection. Exclusion criteria were complete stenosis of the oesophagus hampering marker implantation or the presence of distant metastases leading to palliative treatment. All patients underwent routine staging according to the AJCC/UICC manual (8th edition) [8]. [18F]Fluorodeoxyglucose positron emission tomography (FDG-PET) was preferably scheduled after marker implantation. The investigation was approved by our university's medical ethics committee (EK148042017) and filed with the German registry of clinical trials (DRKS00011886). All patients provided written informed consent.

Fiducial markers

Marker implantation was guided by endoscopic ultrasound (EUS) and performed under conscious sedation and continuous monitoring of vital signs by three experienced endosonographers. One type of flexible, coil-shaped gold marker (VisiCoil™, IBA Dosimetry, Schwarzenbruck, Germany; diameter 0.35 mm, length 5/10 mm) was placed via 22-gauge needles [9]. Two markers were implanted at the upper and lower borders of the tumour, respectively, if both were accessible. An additional marker could be inserted into the healthy oesophagus facing non-circumferential tumours at mid-position. Colour and power Doppler imaging were used to identify a safe insertion window devoid of intervening blood vessels, wherein the endoscopic needle was then inserted submucosally under EUS guidance. After marker release, its location was confirmed using fluoroscopy and the implantation site

inspected for oesophageal bleeding. Patients were monitored for 4 h afterwards.

Pre-treatment imaging

Patients with tumours in the middle or lower third of the oesophagus were immobilised in a vacuum cushion, while a thermoplastic mask covering the head and shoulder region was used in one patient with a tumour affecting the upper third. Patients breathed freely during imaging and subsequent PT. All patients underwent a diagnostic FDG-PET scan (5 mm slice thickness, 4 mm in-plane resolution, Biograph 16; Siemens Healthineers, Erlangen, Germany) and four-dimensional computed tomography (4D CT) for RT planning purposes (pCT; 120 kVp, 2 mm slice thickness, 1 mm in-plane resolution, Somatom Definition AS, Siemens Healthineers). PET-based gross tumour volumes (GTV) comprising all voxels exceeding 40% of the hottest voxel's signal were generated for comparisons of metabolic lesion extent with marker locations [10].

Target volume definition, radiation treatment and chemotherapy

Regions of interest (ROIs) were drawn around fiducial markers on the pCT and isotropically expanded by 3–5 mm to be later projected onto digitally reconstructed radiographs (DRRs) for target verification. GTV delineation was primarily guided by FDG-PET data co-registered to the pCT, but incorporated all available diagnostic information. PET-positive nodes were included in a separate nodal GTV. The clinical target volume (CTV) was derived by expanding the GTV 30 mm longitudinally and 10 mm laterally, with subsequent editing for anatomical boundaries. For tumours demonstrating large mobility on 4D-pCT, the CTVs were further expanded into ITVs by motion-dependent margins ranging from 4 to 10 mm (median: 5). Organs at risk comprising the heart, lungs, spinal cord, stomach, spleen, liver, or kidneys were delineated on the time-averaged pCT.

Treatment plans utilised two to three passively scattered or actively scanned proton fields, delivered with a Proteus PLUS system (IBA Proton Therapy, Louvain-La-Neuve, Belgium) installed at University ProtonTherapy Dresden. Instead of using a PTV, margins around the CTV/ITV allowing for a 3.5% range uncertainty and additional static margins of 2 mm in beam direction and 3 mm laterally were applied. Prescribed doses were 40 GyE or 60–66 GyE for nRCT and definitive RT, respectively, delivered in 2 GyE fractions. Concurrent chemotherapy was administered according to the CROSS protocol and consisted of a paclitaxel/carboplatin doublet delivered once weekly (dosage: 50 mg/m² and AUC2, respectively).

Per-treatment imaging and marker-based target position verification

The gantry at University ProtonTherapy Dresden is equipped with a robotic patient couch with six degrees of freedom (KUKA, Augsburg, Germany), an in-room CT on-rails whose specifications match that of the scanner used for planning purposes, and a gantry-mounted orthogonal X-ray system (resolution approximately 0.2 mm at the isocentre). The latter was used to capture images in treatment position before each fraction using pre-set defaults for tube potential and current-time-product (80 kV/160 mAs for sagittal, 95 kV/50 mAs for coronal views).

In clinical routine, patient setup begins with external alignment of surface marks to the in-room laser system. Thereafter, X-rays are acquired and digitally compared to DRRs derived from the pCT. A setup correction is calculated from a manual registration between the two image pairs based on bony anatomy (VeriSuite, MedCom, Darmstadt, Germany) including shifts and rotations. Finally, for

oesophageal cancer patients, target positioning is verified with the aid of fiducial markers, through their associated ROIs projected onto the DRRs. These should contain the marker to verify its location to within 3–5 mm. Should target misalignment be detected, patient positioning is repeated and/or an in-room control CT (cCT) acquired to investigate its cause.

Retrospective analysis of orthogonal X-ray images

Marker visibility was quantified via the contrast-to-noise ratio (CNR). Two ROIs were constructed around each marker: one containing only the marker projection, the other immediately surrounding, but excluding, it (Fig. 1). The CNR was then computed as the absolute difference in mean pixel values in each ROI divided by their combined standard deviation. Commonly employed minimum CNR thresholds for visibility range from 1 to 2 [11,12].

Markers were manually located in each image pair and their location in 3D reconstructed by triangulation (Algorithm 12.1 in [13]). Two anatomical reference points (vertebral landmarks) per patient were similarly reconstructed, in order to compare findings between projection and tomographic imaging. Triangulation errors were estimated from the distances of closest approach between back-projections of corresponding 2D points (Fig. 1). This measure is primarily sensitive to longitudinal discrepancies, so the 90th percentile of a marker's approach distances in all fractions was assigned as its isotropic triangulation error.

Target displacements relative to the pCT were decomposed into their systematic and random components pro forma in the manner popularised by van Herk et al. [14] (Σ and σ). Displacements in the

three cardinal directions (lateral, sagittal, and longitudinal) were investigated individually, as were the corresponding 3D-vector (Euclidean) distances.

Statistical analysis

Parameter-free tests were used to compare differently grouped variables, since their distributions could not be assumed. Friedman tests were used to compare marker displacements in the three cardinal directions, and Kruskal–Wallis tests to compare unmatched groupings (e.g. marker displacements or CNR for different marker sites). Comparisons of systematic and random components of mobility employ the aforementioned tests on quantities, determined per marker, similar to the ones used to compute the Σ and σ parameters, i.e. individual markers' absolute mean displacements and the standard deviation of individual markers' displacements, respectively (as per [7]). A significance criterion of $p < 0.05$ applies throughout.

Results

Ten consecutive patients were enrolled in the study (Table 1). Eight patients received nRCT, while the remaining two were treated definitively. One (patient 1) was treated for a recurrence of an adenocarcinoma of the gastrooesophageal junction resected two years prior, and the other (patient 9) was not suitable for resection due to a proximal tumour site. The latter patient also received elective treatment of the lower neck nodes up to 40 GyE due to infiltration of the upper oesophageal sphincter. The remain-

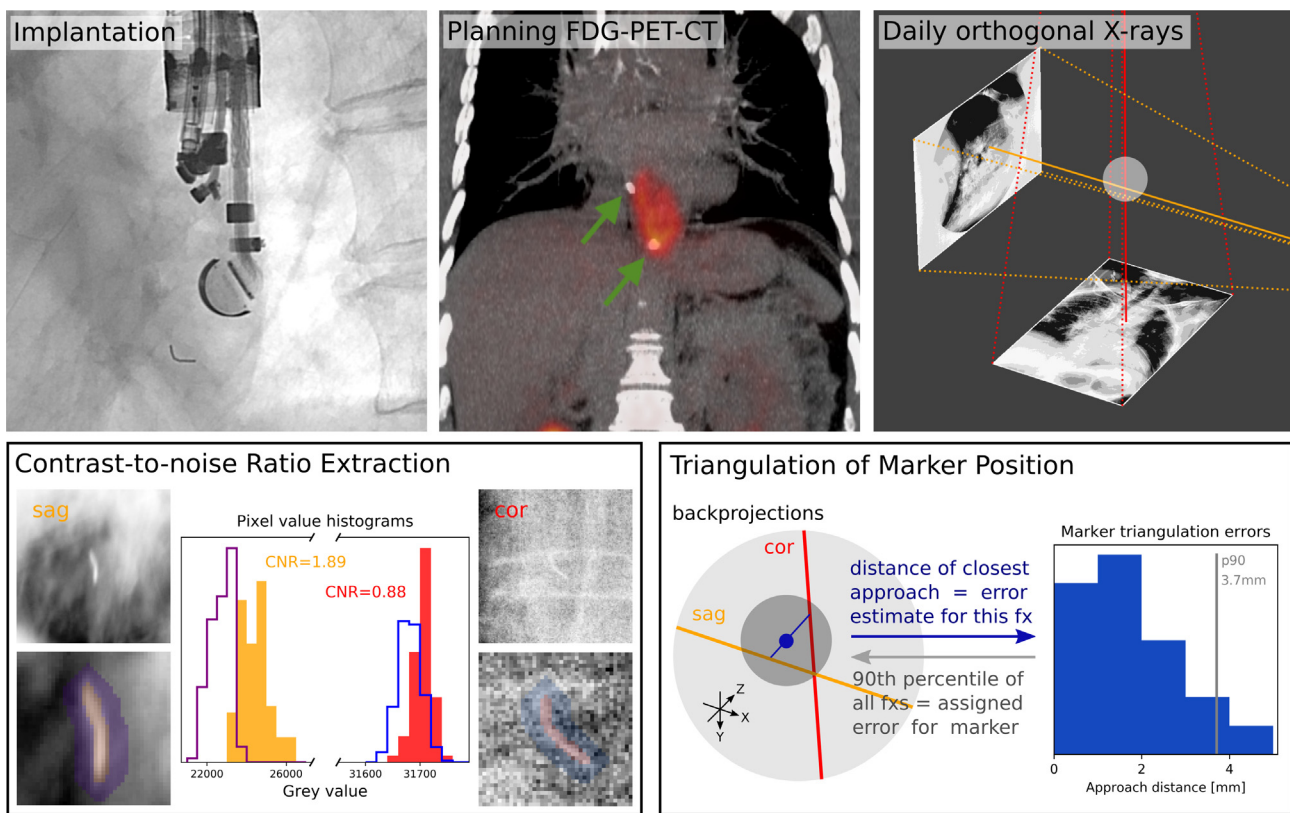


Fig. 1. Overview of marker implantation, imaging techniques and analysis procedures. Top row, left to right: Endoscopic marker implantation showing full range of employed instruments; Correspondence of marker positions and metabolic tumour extent seen in FDG-PET-CT; Geometry of daily X-ray projection imaging. Bottom row: Left: Illustration of CNR extraction using marker and background ROIs for sagittal and coronal views of the same marker achieving good and poor visibility, respectively, based on a visibility criterion of $\text{CNR} > 1$; Right: Illustration of triangulation procedure and determination of one marker's assigned isotropic triangulation error as the 90th percentile of the distribution of distances of closest approach between the back-projections of sagittal and coronal 2D marker positions towards their respective X-ray sources for that marker over all fractions.

Table 1
Patient, tumour, and treatment characteristics.

Patient number	Age [years]	Tumour characteristics [*]		Gross tumour extent [§]		Fiducial markers		Implantation → Imaging		Treatment	
		Location	Classification	Volume [ml]	Length [mm]	Number	Lengths [mm]	pCT [days]	PET [days] [†]	Fractions	cCTs
1	64	lower	rcT1a cN0	9.2	32	2 → 1 [†]	5	4	4	30	2
2	52	lower	cT2 cN1	28.5	40	2	5,10	1	2	20	2
3	58	middle	cT3 cN1	10.4	32	2	10	4	4	20	2
4	62	lower	cT3 cN0	15.0	56	2 → 1 [‡]	5	1	-15	20	2
5	57	middle	cT3 cN0	18.5	40	1	10	2	-34	20	3
6	55	lower	cT3 cN1	69.0	80	2	10	6	6	20	2
7	63	middle	cT3 cN0	27.1	68	2	10	1	-22	20	3
8	67	lower	cT3 cN1	14.1	40	2	10	1.1	1	20	2
9	61	upper	cT3 cN0	5.3	20	2 → 1 ^{††}	10	29	2	33	2
10	74	middle	cT3 cN0	47.7	68	2 ^{††}	10	1	1	20	3

Abbreviations: (p/c)CT, (planning/control) computed tomography; PET, positron emission tomography.

Notes: ^{*}Determined according to AJCC/UICC guidelines. Location refers to affected third of the oesophagus; [§]From GTV delineations; [†]Negative values indicate that acquisition occurred prior to marker implantation; [‡]Proximal marker lost before pCT acquisition; ^{††}Proximal marker became fragmented at implantation and was lost after 7th fraction; ^{†††}Both markers placed at proximal border.

ing patients had tumours affecting the middle ($n = 4$) or lower ($n = 4$) third of the oesophagus.

A total of 19 markers were implanted and since no perioperative complications occurred, the marker and procedure were judged as being safe. In two cases (patients 5 and 10) the distal tumour border was inaccessible by endoscope due to tumour stenosis. One proximal marker fragmented at implantation and was subsequently lost (patient 9).

The median interval between marker implantation and pCT acquisition was 1.5 days (range: 1–29), and the mean GTV extent on the pCT was 24.5 ml (range: 9.2–69.0) in volume and 47.6 mm (range: 20–80) in length.

Three patients received their FDG-PET-CT prior to marker implantation. For the remaining seven cases the PET-CT was obtained with markers in situ, after a median interval of 2.0 days (range: 1–6). Fig. 2 provides an overview of longitudinal marker locations and their correspondence with FDG-PET-derived GTVs.

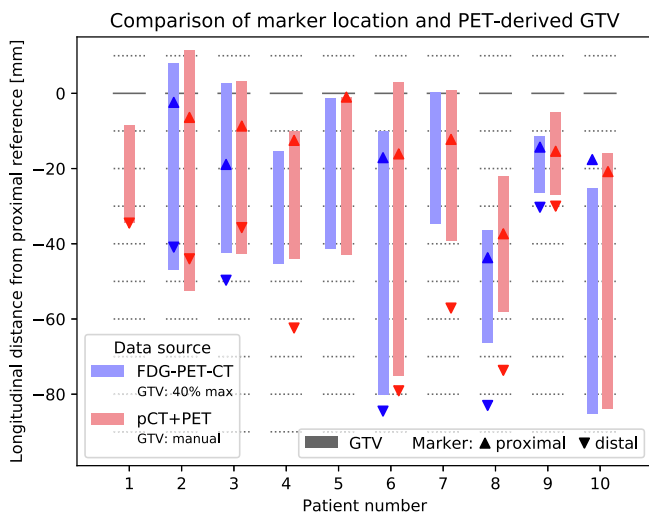


Fig. 2. Overview of longitudinal marker locations (triangles) and GTV lengths (columns). Data extracted from FDG-PET-CT (blue, GTV consists of all voxels whose value exceeds 40% of the lesion's hottest voxel) are compared to data from planning CTs (red, GTV contoured manually using co-registered PET data). Measurements are plotted relative to the proximal anatomical reference point (vertebral landmark). Please note: GTV based on FDG-PET is not shown for patient 1, due to a very weak PET-signal exacerbated by extensive metallic sutures. Some patients did not have a distal marker implanted (5, 10), experienced loss of the proximal marker before imaging (1), or had their PET acquired before implantation (4,5,7).

The mean distance between marker positions and corresponding GTV borders was -5.4 ± 8.1 mm (range: -21.5 – 7.5), with negative values indicating markers located more distally.

X-ray pairs utilised for patient positioning could be retrieved for 211/223 fractions and the number of cCTs per patient ranged from 2 to 3. Markers were easily detected in (PET-)CT image sets, while visibility in X-ray images was generally limited but mostly sufficient. Markers were completely undetectable in sagittal views of the patient whose very proximally located tumour required immobilisation with a thermoplastic mask. Consequently, the number of analysable marker projection pairs was reduced to 307 out of a possible 446 if all patient had received two markers, which remained stable and visible throughout.

The overall mean CNR was 1.5 ± 0.5 (range: 0.2–3.2) with 508 and 90 out of 614 marker projections satisfying a visibility criterion of $\text{CNR} > 1$ and $\text{CNR} > 2$, respectively. Mean CNRs were 1.5 ± 0.5 for sagittal and 1.5 ± 0.5 for coronal projections ($p = 0.8$), while values of 1.7 ± 0.3 , 1.7 ± 0.5 , and 1.4 ± 0.4 were achieved with markers located in the upper, middle and lower third of the oesophagus, respectively ($p < 0.01$).

Assigned triangulation errors per marker ranged from 0.8 to 4.8 mm (mean: 2.4 ± 1.2) and showed a dependence on marker site with mean values of 3.1 ± 1.0 mm for the lower third of the oesophagus and 1.6 ± 0.9 mm for the others ($p = 0.01$).

Fig. 3 shows the aggregate distributions of marker displacements alongside summary statistics. Systematic error components (Σ) measured 2.6, 2.0, and 4.0 mm in the lateral, sagittal, and axial directions, respectively. The corresponding random components (σ) measured 3.0, 2.0, and 3.2 mm. Differences between the directions failed to reach significance for the systematic component ($p = 0.3$), but did so for the random one ($p < 0.05$). No significant differences in mobility were found with regard to marker location.

Euclidean displacement exceeded 5 and 10 mm in 181 and 57 out of 307 cases, respectively. The most extreme instance of marker displacement is shown in Fig. 4 and features the proximal and distal marker displaced by 17 and 31 mm, respectively. This prompted the acquisition of a cCT, which revealed an overlap of the planned and actual GTVs of merely 4% (Jaccard index: 0.02). The dosimetric impact would have been a reduction in the mean and near-min (D98%) doses to the GTV by 6% and 47%, respectively.

Two proximal markers of 5 mm length became dislodged before or during treatment (patients 1, 4). Fig. 5 shows the sole instance of progressive marker migration, wherein it travelled more than 10 mm in 10 fractions and was simultaneously deformed. No other cases exhibited systematic marker migration and all marker losses occurred abruptly.

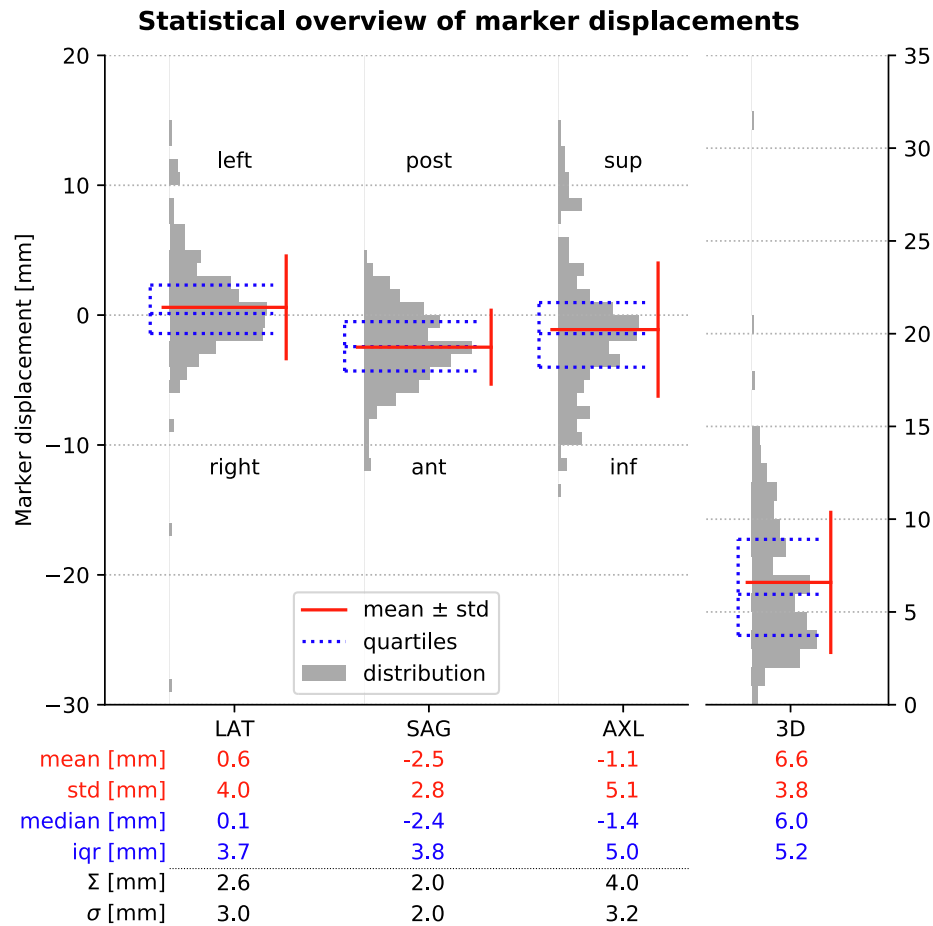


Fig. 3. Distributions of inter-fractional marker displacements relative to their planned position in each of the cardinal directions, as well as their Euclidean combination. Distributions are shown as histograms (grey, 1 mm binning). Summary statistics are drawn as coloured lines and printed underneath. Σ and σ refer to the decomposition of mobility measurements into systematic and random components as per [14]. Abbreviations: LAT, lateral; SAG, sagittal; AXL, axial; 3D, 3D vector (Euclidean) distance; post, posterior; ant, anterior; sup, superior; inf, inferior; std, standard deviation; iqr, inter-quartile range.

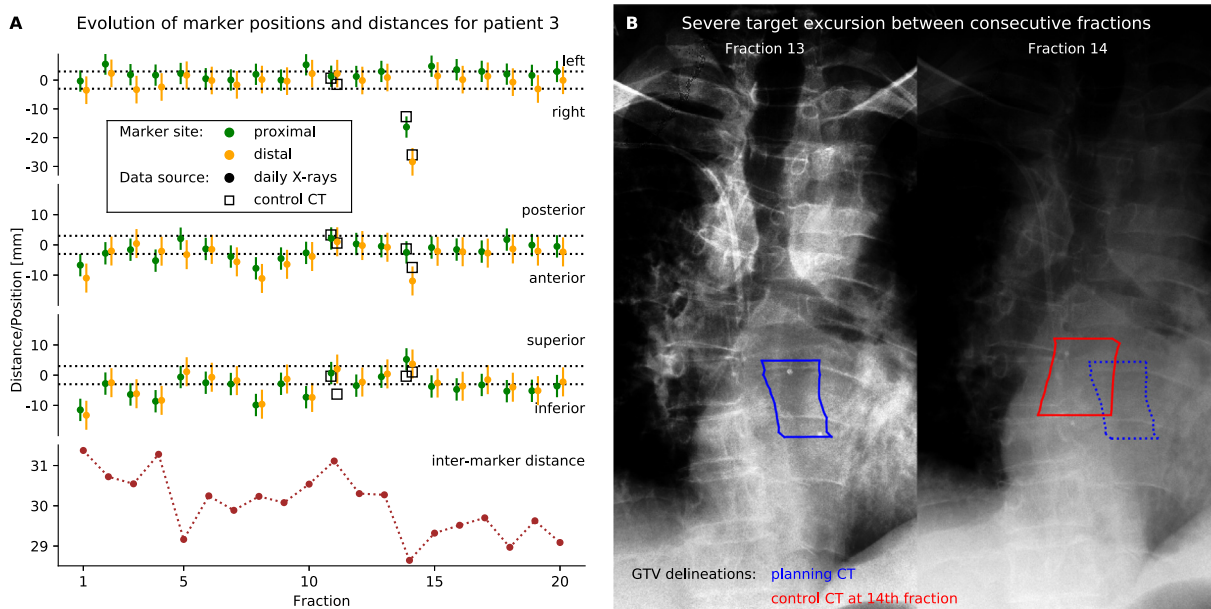


Fig. 4. Marker positions over the course of treatment for a patient showing severe target displacement at one fraction, as well as detailed views of the latter. (A) Marker positions in cardinal directions for each fraction, as well as the corresponding Euclidean inter-marker distances. Dotted horizontal lines indicate the nominal 3 mm verification threshold. (B) Coronal views for fractions 13 and 14 showing pronounced excursion of both markers to the right. Projections of GTVs delineated on the planning CT and a control CT are superimposed for comparison.

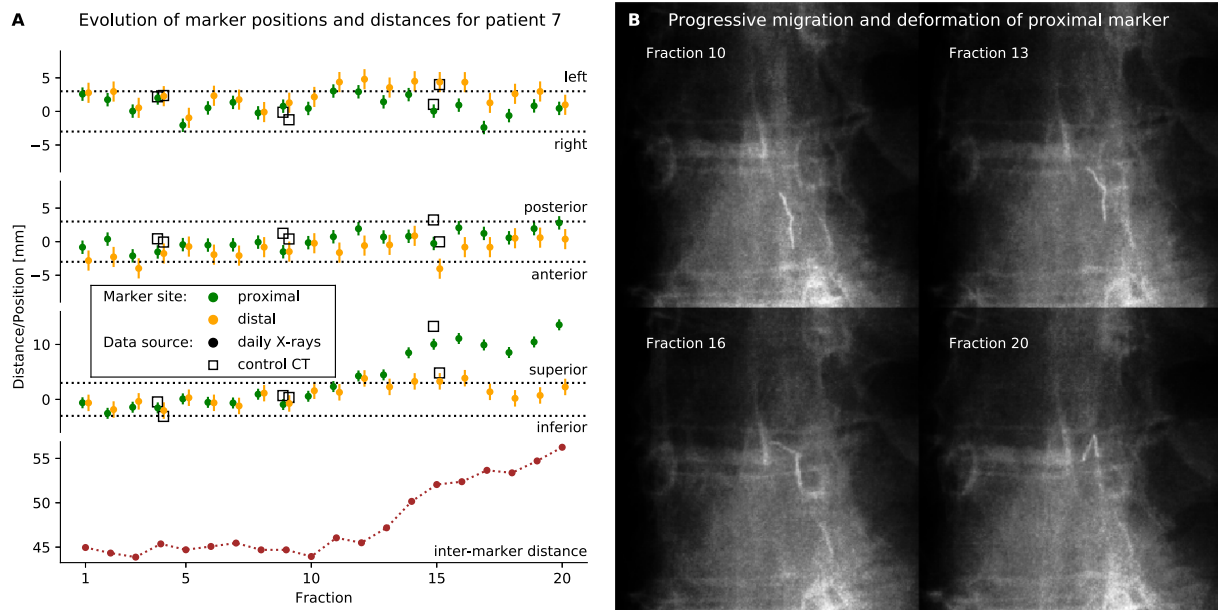


Fig. 5. Marker positions over the course of treatment for a patient, whose proximal marker underwent progressive migration and deformation, as well as detailed views of the latter. (A) Marker positions in cardinal directions for each fraction, as well as the corresponding Euclidean inter-marker distances. Dotted horizontal lines indicate the nominal 3 mm verification threshold. (B) Coronal views of the proximal marker for fractions 10, 13, 16, and 20. Each view is centred on the interface of thoracic vertebrae 5 and 6.

Discussion

Correct target positioning has always played a crucial role in RT, in particular for tumours originating from highly mobile organs, but it is becoming even more critical as efforts to increase dose conformality and reduce physical planning margins are spreading. It is of special importance in PT whose physical characteristics render dose deposition strongly susceptible to anatomical changes. Oesophageal carcinoma are difficult to visualise natively using the imaging equipment available at most PT centres. A recent survey among European centres identified 2D X-ray as the dominant modality and 3D cone-beam CT (CBCT) as on the rise [15]. Both modalities are capable of providing bony-anatomy based patient positioning, but have limited ability to visualise the oesophagus. In the case of 3D (CB)CT visualisation of the oesophagus is technically achievable in some cases, but the lack of soft tissue contrast makes direct target-to-target matching very difficult such that reliable surrogates need to be found [16]. All three imaging modalities will thus benefit greatly from radiopaque demarcations of the target volume in order to position patients accurately and precisely.

This investigation represents the first detailed utility analysis of VisiCoil™ fiducial markers in neoadjuvant or definitive proton RCT of oesophageal carcinoma. Marker implantation proceeded without complications and all markers of the longer type (10 mm) remained stable throughout treatment. Marker visibility was oftentimes limited but mostly sufficient and marker positions could be triangulated for all but one patient.

We assessed the discrepancies between tumour extent highlighted by FDG-PET-CT and that demarcated by the fiducial marker. It is known, that the addition of FDG-PET to CT-based treatment planning has enabled more accurate definition of both primary and nodal GTVs in oesophageal cancer [17]. Foley et al. [18] found improved assessment of local disease extent by EUS, and strongly recommend combining information from FDG-PET and EUS with the pCT. As shown in this study, fiducial markers placed under EUS-guidance support this approach by making endoscopic findings available on projective or tomographic X-ray imaging. Possible

explanations for the observed differences may arise from the mobility of the oesophagus, the lengths of the fiducial markers, and from the technique of marker implantation during EUS.

Marker visibility could be substantially improved through the optimisation of X-ray imaging parameters beyond the current clinical settings, as detailed by Chen et al. [11] in the context of prostate RT. They used an anthropomorphic phantom and determined the optimal ratio of CNR to entrance skin exposure for varying combinations of tube potential and current-time-product for individual projection angles. The optimal settings determined through such a procedure are likely not transferable to all patients, but could serve as a starting point for patient-specific optimisation.

Fiducial marker mobility measurements in our study were generally in good agreement with those by Jin et al. [7], who used a variety of fiducial markers and frequent CBCT to study inter-fractional motion of oesophageal tumours. For their entire cohort of 65 markers (31 in the distal oesophagus) they measured Σ as 2.9, 2.2, and 4.1 mm, for the lateral, sagittal, and axial directions, respectively, and σ as 2.4, 1.8, and 2.4 mm. They report significant differences in both systematic and random components of movement when comparing cardinal directions, with highest mobility in the longitudinal direction. It is most likely due to the moderate sample size, that such differences could only be demonstrated for the random component in our study. Overall it is encouraging to see that 3D and orthogonal-2D imaging produce very compatible measurements of Σ and σ .

In our study, the distributions of marker displacements show some prominent outliers, which partially stem from fractions where positioning was ultimately established by cCT without repeating X-ray imaging. There is a sizeable systematic shift in the sagittal direction whose underlying cause has yet to be understood.

No systematic marker migrations were observed apart from the highlighted case (patient 7), in which a steady increase in inter-marker distance driven by the proximal marker moving upward was found. The cause of this migration is unclear, with the FDG-PET-CT obtained in the fourth week of RCT revealing some degree

of tumour regression. A decrease in inter-marker distance has not been observed even in cases where pronounced tumour shrinkage could be demonstrated on follow-up imaging or in resection specimen. Systematic migration of individual markers was also not observed and the two instances of marker losses during treatment were both abrupt, such that poor marker implantation could not be mistaken for profound anatomical changes.

Some clinicians fear that metallic markers can cause severe dose shadows in ion beams. Indeed, several simulation and measurement studies (e.g. [19–21]) have shown dose deficits of up to 80%, depending on marker dimensions, material, orientation and position relative to the beams and their respective Bragg peaks. This has prompted the development of novel marker materials (e.g. carbon and liquid fiducial markers [22]), as well as the introduction of reduced material markers, such as VisiCoil™. Two studies included this marker type and diameter, measuring dose perturbations in mono-energetic proton or carbon ion beams [19] and at different positions in a spread-out proton Bragg peak [20]. Neither study reports observable dose perturbations for the 0.35 mm diameter VisiCoil™ marker. Machiels et al. [23] compared this calibre of VisiCoil™ to solid gold markers of similar outer dimensions finding superior stability for the helical design, thereby demonstrating that the favourably low material budget does not sacrifice stability. They recommend marker lengths greater than 5 mm for optimal stability, which is in line with our findings.

Another potential risk of metallic fiducial markers is a reduction in diagnostic accuracy through the artefacts they cause. Streak artefacts on CT are the most obvious concern, which, at least for the size of marker employed in this study, did not cause noticeable problems. Implanted markers might also result in overestimated FDG-PET signals via physical (CT artefacts impacting attenuation correction) or biological (inflammatory reactions) mechanisms. Neither of these phenomena was observed in this study. Unquestionably, marker implantation must be scheduled and performed in a way, which does not delay subsequent diagnostic work-up, and treatment preparation and delivery, perhaps adding a slight complication to clinical workflows.

In conclusion, in this relatively small pilot cohort implanted fiducial markers were shown to be a valuable aid in target delineation and a helpful tool for target-centric positioning verification in oesophageal carcinoma.

Conflict of interest

None.

References

- [1] Van Hagen P, Hulshof MCCM, Van Lanschot JJB, Steyerberg EW, Van Berge Henegouwen MI, Wijnhoven BPL, et al. Preoperative chemoradiotherapy for esophageal or junctional cancer. *N Engl J Med* 2012;366:2074–84. <https://doi.org/10.1056/NEJMoa1112088>.
- [2] Shapiro J, Van Lanschot JJB, Hulshof MCCM, Van Hagen P, Van Berge Henegouwen MI, Wijnhoven BPL, et al. Neoadjuvant chemoradiotherapy plus surgery versus surgery alone for oesophageal or junctional cancer (CROSS): long-term results of a randomised controlled trial. *Lancet Oncol* 2015;16:1090–8. [https://doi.org/10.1016/S1470-2045\(15\)00040-6](https://doi.org/10.1016/S1470-2045(15)00040-6).
- [3] Xi M, Xu C, Liao Z, Chang JY, Gomez DR, Jeter M, et al. Comparative outcomes after definitive chemoradiotherapy using proton beam therapy versus intensity modulated radiation therapy for esophageal cancer: a retrospective, single-institutional analysis. *Int J Radiat Oncol Biol Phys* 2017;99:667–76. <https://doi.org/10.1016/j.ijrobp.2017.06.2450>.
- [4] Lin S, Merrell K, Shen J, Verma V, Correa A, Wang L, et al. Multi-institutional analysis of radiation modality use and postoperative outcomes of neoadjuvant chemoradiotherapy for esophageal cancer. *Radiother Oncol* 2017;123:376–81. <https://doi.org/10.1016/j.radonc.2017.04.013>.
- [5] Dieleman E, Senan S, Vincent A, Lagerwaard F, Slotman B, Van Sörnsen de Koste J. Four-dimensional computed tomographic analysis of esophageal mobility during normal respiration. *Int J Radiat Oncol Biol Phys* 2007;67:775–80. <https://doi.org/10.1016/j.ijrobp.2006.09.054>.
- [6] Cohen R, Paskalev K, Litwin S, Price R, Feigenberg S, Konski A. Esophageal motion during radiotherapy: quantification and margin implications. *Dis Esophagus* 2010;23:473–9. <https://doi.org/10.1111/j.1442-2050.2009.01037.x>.
- [7] Jin P, Van der Horst A, De Jong R, Van Hooff J, Kamphuis M, Van Wieringen N, et al. Marker-based quantification of interfractional tumor position variation and the use of markers for setup verification in radiation therapy for esophageal cancer. *Radiother Oncol* 2015;117:412–8. <https://doi.org/10.1016/j.radonc.2015.10.005>.
- [8] Amin MB, Edge S, Greene F, Byrd DR, Brookland RK, Washington MK, editors. *AJCC Cancer Staging Manual*. New York: Springer; 2017.
- [9] DiMaio C, Nagula S, Goodman K, Ho A, Markowitz A, Schattner M, et al. EUS-guided fiducial placement for image-guided radiation therapy in GI malignancies by using a 22-gauge needle (with videos). *Gastrointest Endosc* 2010;71:1204–10. <https://doi.org/10.1016/j.gie.2010.01.003>.
- [10] Lu J, Sun X, Yang X, Tang X, Qin Q, Zhu H, et al. Impact of PET/CT on radiation treatment in patients with esophageal cancer: A systematic review. *Crit Rev Oncol Hematol* 2016;107:128–37. <https://doi.org/10.1016/j.critrevonc.2016.08.015>.
- [11] Chen Y, O'Connell J, Ko C, Mayer R, Belard A, McDonough J. Fiducial markers in prostate for kV imaging: quantification of visibility and optimization of imaging conditions. *Phys Med Biol* 2012;57:155–72. <https://doi.org/10.1088/0031-9155/57/1/155>.
- [12] Luo W, Yoo S, Wu QJ, Wang Z, Yin F. Analysis of image quality for real-time target tracking using simultaneous kV-MV imaging. *Med Phys* 2008;35:5501–9. <https://doi.org/10.1118/1.3002313>.
- [13] Hartley R, Zisserman A. *Multiple View Geometry in Computer Vision*. 2nd ed. New York: Cambridge University Press; 2004.
- [14] Van Herk M. Errors and margins in radiotherapy. *Semin Radiat Oncol* 2004;14:52–64. <https://doi.org/10.1053/j.semradiol.2003.10.003>.
- [15] Bolsi A, Peroni M, Amelio D, Dasu A, Stock M, Toma-Dasu I, et al. Practice patterns of image guided particle therapy in Europe: A 2016 survey of the European Particle Therapy Network (EPTN). *Radiother Oncol* 2018;128:4–8. <https://doi.org/10.1016/j.radonc.2018.03.017>.
- [16] Hawkins MA, Aitken A, Hansen VN, McNair HA, Tait DM. Cone beam CT verification for oesophageal cancer - impact of volume selected for image registration. *Acta Oncol* 2011;50:1183–90. <https://doi.org/10.3109/0284186X.2011.572912>.
- [17] Schreurs LMA, Busz DM, Paardekooper GMRM, Beukema JC, Jager PL, Van der Jagt EJ, et al. Impact of 18-fluorodeoxyglucose positron emission tomography on computed tomography defined target volumes in radiation treatment planning of esophageal cancer: reduction in geographic misses with equal inter-observer variability: PET/CT improves esophageal target definition. *Dis Esophagus* 2010;23:493–501. <https://doi.org/10.1111/j.1442-2050.2009.01044.x>.
- [18] Foley KG, Morgan C, Roberts SA, Crosby T. Impact of positron emission tomography and endoscopic ultrasound length of disease difference on treatment planning in patients with oesophageal cancer. *Clin Oncol (R Coll Radiol)* 2017;29:760–6. <https://doi.org/10.1016/j.clon.2017.07.014>.
- [19] Habermehl D, Henkner K, Ecker S, Jäkel O, Debus J, Combs S. Evaluation of different fiducial markers for image-guided radiotherapy and particle therapy. *J Radiat Res* 2013;54:i61–8. <https://doi.org/10.1093/jrr/rrt071>.
- [20] Giebler A, Fontenot J, Balter P, Ciangaru G, Zhu R, Newhauser W. Dose perturbations from implanted helical gold markers in proton therapy of prostate cancer. *J Appl Clin Med Phys* 2009;10:2875.
- [21] Newhauser W, Fontenot J, Koch N, Dong L, Lee A, Zheng Y, et al. Monte Carlo simulations of the dosimetric impact of radiopaque fiducial markers for proton radiotherapy of the prostate. *Phys Med Biol* 2007;52:2937–52. <https://doi.org/10.1088/0031-9155/52/11/001>.
- [22] Scherman Rydhög J, Perrin R, Jølck RI, Gagnon-Moisan F, Larsen KR, Clementsen P, et al. Liquid fiducial marker applicability in proton therapy of locally advanced lung cancer. *Radiother Oncol* 2017;122:393–9. <https://doi.org/10.1016/j.radonc.2016.12.027>.
- [23] Machiels M, Van Hooff J, Jin P, Van Berge Henegouwen MI, Van Laarhoven HM, Alderliesten T, et al. Endoscopy/EUS-guided fiducial marker placement in patients with esophageal cancer: a comparative analysis of 3 types of markers. *Gastrointest Endosc* 2015;82:641–9. <https://doi.org/10.1016/j.gie.2015.03.1972>.